

First-principles investigation of Mg segregation at $\Sigma = 11(113)$ grain boundaries in Al

This article has been downloaded from IOPscience. Please scroll down to see the full text article.

2005 J. Phys.: Condens. Matter 17 4301

(<http://iopscience.iop.org/0953-8984/17/27/006>)

View [the table of contents for this issue](#), or go to the [journal homepage](#) for more

Download details:

IP Address: 129.252.86.83

The article was downloaded on 28/05/2010 at 05:14

Please note that [terms and conditions apply](#).

First-principles investigation of Mg segregation at $\Sigma = 11(113)$ grain boundaries in Al

Xiaoguang Liu¹, Xiaowei Wang^{1,4}, Jingyang Wang^{1,2} and Hongyan Zhang³

¹ Shenyang National Laboratory for Materials Science, Institute of Metal Research, Chinese Academy of Sciences, 72 Wenhua Road, Shenyang 110016, People's Republic of China

² International Centre for Materials Physics, Institute of Metal Research, Chinese Academy of Sciences, Shenyang 110016, People's Republic of China

³ Department of MIME, University of Toledo, Toledo, OH 43606, USA

Received 30 January 2005, in final form 18 May 2005

Published 24 June 2005

Online at stacks.iop.org/JPhysCM/17/4301

Abstract

The preferred site of Mg segregation at $\Sigma = 11(113)$ grain boundaries in Al and the effects of Mg segregation on grain boundary cohesion have been investigated through first-principle pseudopotential total energy calculations. The results show that the Mg atom prefers to occupy the 'looser' site at the grain boundary of Al but not the 'tighter' site. Furthermore, on basis of the thermodynamic theory of Rice and Wang, we have studied the effect of Mg segregation on the grain boundary cohesion of Al. Our total energy calculations show that Mg behaves as an embrittler. Additionally, the cohesive energies for a pure Al boundary and an Al boundary with Mg segregation have been calculated in this paper. The calculated results indicate that the cohesion of an Al grain boundary with Mg segregation is weaker than that of a pure Al grain boundary. The total charge density of the grain boundary also demonstrates that the Mg atom forms weaker metallic bonds with neighbouring Al atoms in the grain boundary region.

1. Introduction

Al alloys with Mg as the major alloying element constitute a group of non-heat-treatable alloys with medium strength, high ductility, excellent corrosion resistance and weldability [1, 2]. However, the segregation of Mg to grain boundaries may adversely affect the performance of these materials. Na *et al* [3] observed that grain boundary cracking of Al–2.9% Mg alloy occurred and accelerated when Mg atoms segregated to the grain boundaries via Cottrell atmospheres around dislocations under cyclic stressing. Song *et al* showed that the crack propagation velocity of 7050 Al alloy, tested in humid air, was directly proportional to

⁴ Author to whom any correspondence should be addressed.

grain boundary Mg segregation as measured by Auger electron spectroscopy (AES) [4]. Using molecular statics simulations, Namila *et al* calculated the grain boundary energy for various [110] symmetric tilt grain boundaries with one Mg atom placed at or near a grain boundary [5]. Liu and Adams investigated Mg segregation in various grain boundaries of Al–10% Mg alloys at hot working temperatures by the Monte Carlo technique. The effect on decohesion of grain boundaries due to Mg segregation was found to be a modest (10–35%) reduction in fracture energy compared to the fracture energy in pure Al [6]. Investigations of the bonding characteristics of the Mg atom with its neighbouring Al atoms in the boundary region, which are of crucial importance in understanding the granular embrittlement of Al–Mg alloys, are absent from previous works. The investigation of the preferred sites of Mg atoms at a boundary region could provide an electronic level understanding of the mechanism of Mg segregation and the bonding strength of grain boundaries. This can be accomplished by investigating the Mg behaviour at the Al grain boundaries by the means of first-principles method.

In this study, the interaction of Mg with Al atoms at grain boundaries was investigated by first-principles pseudopotential total energy calculations. The preferred site of Mg segregation at a boundary was studied by calculating the energy differences when putting Mg atoms in several types of sites on a $\Sigma = 11(113) 129.52^\circ$ symmetric tilt boundary, one at a time, with the energy of Mg dissolved in bulk Al taken as the reference energy. The effect of Mg segregation on the cohesion of a boundary was studied by comparing the cohesive energy of a pure Al boundary and that of a boundary with Mg segregation. The interatomic bonding characteristics were illustrated by total charge density distribution.

2. Computation details and boundary structure

The calculations were performed using the CASTEP code, which is a plane-wave pseudopotential total energy computation method based on density functional theory [7]. The electronic exchange–correlation energy was treated using the generalized gradient approximation (GGA-PW91) [8]. Interactions of electrons with ion cores were represented by the Vanderbilt-type ultrasoft pseudopotential for Al [9] and norm-conserving pseudopotential for Mg generated using the Kleinman–Bylander representation [10]. Compared with the norm-conserving pseudopotential, the ultrasoft pseudopotential yielded better results for Al: for instance, an equilibrium lattice constant of 3.959 Å and a grain boundary energy of 208 mJ m⁻², which are in a better agreement with another *ab initio* result of 201 mJ m⁻² by Wright and Atlas [11]. The plane-wave basis set's cut-off was set as 450 eV for all cases, which was sufficient to lead to a reasonable convergence for calculating total energy and forces acting on the atoms. The special point sampling integration over the Brillouin zone was employed by using the Monkhorst–Pack method with a $3 \times 9 \times 1$ special *k*-point mesh [12]. Geometry optimization was done by using the Broyden–Fletcher–Goldfarb–Shanno (BFGS) minimization scheme [13]. The tolerances for geometry optimization were set as the difference on total energy within 5×10^{-6} eV/atom, maximum ionic Hellmann–Feynman force within 0.01 eV Å⁻¹, maximum ionic displacement within 5×10^{-4} Å, and maximum stress within 0.02 GPa.

The grain boundary structure was modelled in a supercell that was repeated periodically in three dimensions to represent the extended solid. In the present case, the supercell contained two grain boundaries so that periodicity was maintained along the direction perpendicular to the boundary plane. Figure 1 shows the supercell of 44 atoms adopted with a pair of $\Sigma = 11(113)$ boundaries. The orientation of the grain boundary is similar to the one studied in Wright *et al*'s work [11]. The boundary was chosen because it was a stable structure identified by

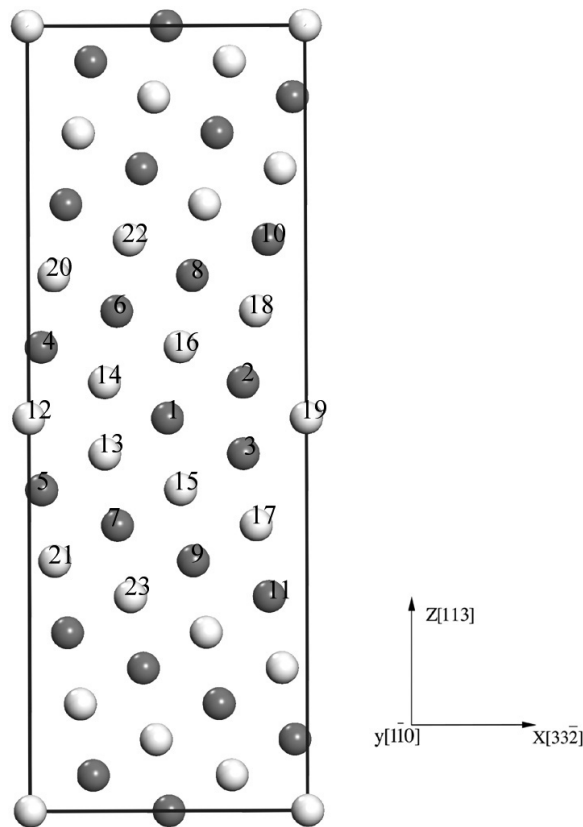


Figure 1. 44-atom supercell for the $\Sigma = 11(113)$ symmetric tilt boundary. The structure repeats after two layers of atoms along the $[110]$ direction and atoms in different layers are designated by white and grey circles, which represent atoms in layers $y = 0$ and 0.5 , respectively.

Mill *et al* using the embedded-atom method (EAM) calculation and high-resolution transmission-electron microscopy (HRTEM) observation [14] and by Wright *et al* using density-functional calculations [11]. Three types of sites were chosen: type I sites (1, 12, and 19) in the plane of the boundary are ‘looser’ sites; type II sites (2, 3, 13, and 14) in the layers on either side of the boundary plane are ‘tighter’ sites; and type III sites (4, 5, 15, and 16) in the next layers are normal sites, whose environment is bulk-like [15]. The ‘looser’ and ‘tighter’ sites mean that their atomic environment is not bulk-like, which forces atoms occupying the sites to accept longer and shorter near-neighbour bonds than they would prefer energetically. Calculations for segregation energy were performed for the three types of sites with one Mg atom substitution. In each case, one Mg atom is substituted into various sites of a boundary, and a symmetrical equivalent substitution is made at the other boundary.

The lattice parameters and atomic positions of the grain boundaries and free surfaces were fully optimized along the direction perpendicular to the boundary plane in this study. When the effect of Mg on the cohesion of grain boundaries in Al was considered, the difference in binding energies of the Mg in the free surface and in grain boundary environments was very small. Therefore, to obtain reliable values, the free surface and grain boundary systems must be equally treated. The atomic structures of the free surfaces and grain boundaries should also be optimized for the cases with and without Mg atom substitution. For this reason, the same set

Table 1. Calculated segregation energies (meV) with one substitutional Mg atom occupying various types of sites near and in a boundary.

	Site I	Site II	Site III
Segregation energy	−185	−2	−70

of numerical parameters was used in the CASTEP calculations for both grain boundaries and free surfaces. The calculated atomic configurations and electronic structures were analysed for the fully relaxed systems.

3. Results and discussion

3.1. The preferred site of Mg in the boundary region

3.1.1. Analysis of the segregation energy. The segregation energy can be defined as the difference in total energy between the cell with one Mg atom being substituted in the boundary and the cell with one Mg atom in the bulk solid solution. In order to minimize computational errors, two Mg atoms were substitutionally placed in a 44-atom bulk face-centred cubic (fcc) supercell of the same size and equivalent shape as that in figure 1 to obtain the energy of dissolved Mg [15]. The segregation energy of the substituted Mg atom at the grain boundary is given by

$$\Delta E = (1/2)[E_{\text{bound}}^{\text{Mg}} - E_{\text{bound}}^{\text{Al}}] - (1/2)[E_{\text{bulk}}^{\text{Mg}} - E_{\text{bulk}}^{\text{Al}}] \quad (1)$$

where $E_{\text{bound}}^{\text{Mg}}$ and $E_{\text{bound}}^{\text{Al}}$ represent the total energy of the boundary supercell with Mg segregation and that of the pure Al boundary supercell, respectively. $E_{\text{bulk}}^{\text{Al}}$ is the total energy of the 44-atom bulk fcc Al supercell, and $E_{\text{bulk}}^{\text{Mg}}$ is the total energy of the same bulk fcc supercell with two Mg substituted. The segregation energies of the three boundary configurations are given in table 1. The segregation energies for the ‘looser’, ‘tighter’ and normal sites are −185, −2, and −70 meV, respectively. The segregation energy of a ‘looser’ site yields the largest absolute value of energy. This indicates that the Mg atom prefers to occupy a ‘looser’ site in the plane of the grain boundary in Al.

3.1.2. The local strain relaxation. The preferred sites of Mg in the boundary region can be explained by the local strain relaxation. The interatomic distance between atoms 2 and 3 as well as atoms 13 and 14, as shown in figure 1, across the boundary plane provides a clue to the distortion due to the grain boundary. For a pure Al boundary the distance is 2.660 Å, compared to the normal nearest-neighbour distance of 2.800 Å in fcc Al. This obviously provokes a repulsive response between the two Al atoms, and leads to an expansion perpendicular to the boundary plane. When an Al atom at a ‘looser’ site (i.e. type I site) is substituted by a Mg atom, the interatomic distance increases to 2.730 Å, which is much closer to the interatomic distance in bulk Al (2.800 Å) than that in pure Al boundary (2.660 Å). Furthermore, the distances between Mg and its neighbouring atoms are 2.906 Å for atom 2, 2.943 Å for atom 13 and 2.968 Å for atom 15, respectively. The bond lengths are approximately equal to the summation of the Al atomic radius (1.400 Å) and Mg atomic radius (1.559 Å), which is 2.959 Å. When a ‘tighter’ site (i.e. type II site) is substituted by one Mg atom, the distance between atom 3 and Mg becomes 2.790 Å. This is smaller than the summation of Al and Mg radii (2.959 Å), and therefore, a repulsive interaction between the two atoms still exists. When a normal site (i.e. type III site, such as atom 5) is occupied by one Mg atom, the distance between atom 2 and 3 becomes 2.703 Å. This indicates that a Mg at a normal site

Table 2. Calculated binding energy differences (eV) with a Mg in an Al grain boundary in a free surface environment.

	ΔE_b	ΔE_s	ΔE_{GB}
Mg substitution	-32.703	-32.825	0.122

relaxes less local strain than it does at a ‘looser’ site. Furthermore, the neighbouring atoms around the Mg atom are also relaxed a little. For instance, the distances between the Mg and its neighbouring atoms are 2.888 Å for atom 7, 2.873 Å for atom 12, 2.969 Å for atom 13 and 2.951 Å for atom 21, respectively. Therefore, it can be concluded from the above analysis that a Mg atom occupying a ‘looser’ site relaxes the bond lengths to a more energetically preferred local configuration. A ‘looser’ site in the plane of the grain boundary (i.e. type I site) is preferable for Mg segregation, while a ‘tighter’ or a normal site is not.

3.2. Effect of Mg on the grain boundary cohesion of Al

The effect of Mg on grain boundary cohesion of Al was investigated based on the Rice and Wang thermodynamics theory [16]. The theory suggests that the potency of an impurity in reducing the ‘Griffith work’ of a brittle boundary separation is a linear function of the difference in binding energies (ΔE_{GB}). If an impurity occupies a substitutional position (i.e. replaces a host atom) at the grain boundary core (atom 1 in this case), its embrittlement potency is then determined by the difference in binding energies.

$$\Delta E_{GB} = \Delta E_b - \Delta E_s \quad (2)$$

ΔE_b and ΔE_s are defined as

$$\Delta E_b = \Delta E_b^{Mg} - \Delta E_b^{Al} \quad (3)$$

$$\Delta E_s = \Delta E_s^{Mg} - \Delta E_s^{Al}. \quad (4)$$

Here ΔE_b^{Mg} and ΔE_b^{Al} are the total energies of the grain boundary with and without the Mg atom substitution, respectively. ΔE_s^{Mg} and ΔE_s^{Al} are the total energies of the free surfaces with and without the Mg atom substitution, respectively. In equation (2), if $\Delta E_{GB} > 0$, Mg would tend to segregate to a free surface rather than a grain boundary, and thus there would be embrittling at the grain boundary.

The calculated energies are listed in table 2. ΔE_{GB} is 0.122 eV with Mg substitution, which clearly indicates that the Mg atom serves as an embrittler. This implies that Mg segregation may lead to cracking of the grain boundary in Al–Mg alloy.

The effect of Mg atoms on the grain boundary cohesion of Al can also be understood through a cohesive energy analysis, which is a measure of the strength of the forces that bind atoms together in the solid state. The cohesive energy is defined as the total energy of the constituent atoms at infinite separation minus the total energy of the supercell. The calculated cohesive energies for a pure Al boundary and an Al boundary with Mg segregation are listed in table 3. The cohesive energies are 4.157 eV/atom for the Al boundary with Mg segregation, and 4.266 eV/atom for the pure Al boundary. It is noted that the cohesive energy of the Mg-substituted boundary is smaller than that of the pure Al boundary. This indicates that Mg segregation increases the embrittlement of the grain boundary.

3.3. Charge density distribution

In first-principles computations, the charge density is always used to discuss interatomic interactions. Figures 2(a) and (b) show the total charge densities in layers $y = 0$ and 0.5,

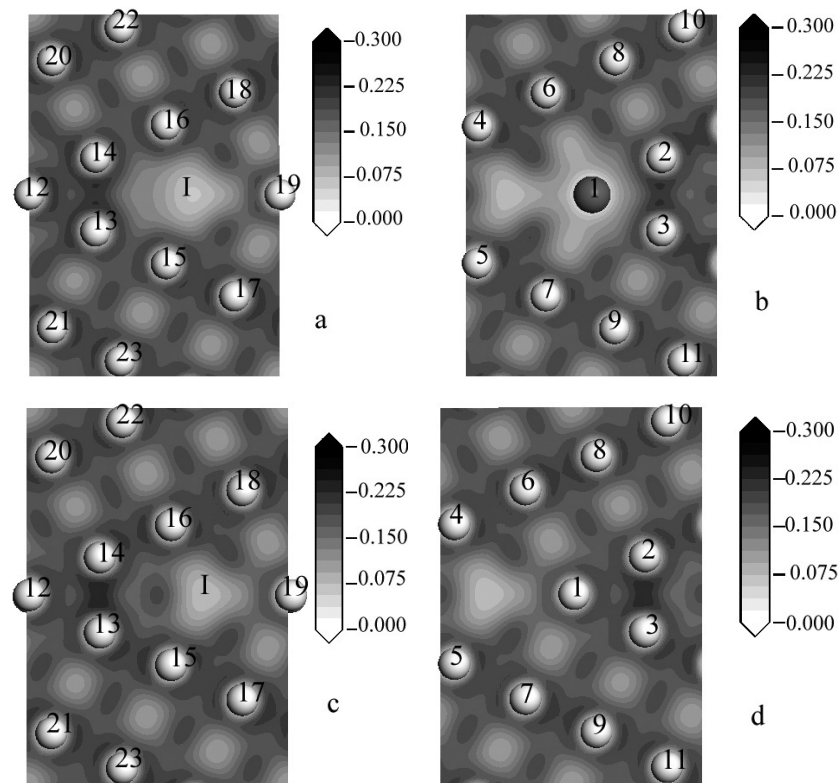


Figure 2. Slices of the total charge densities in planes perpendicular to the $[1\bar{1}0]$ direction for $\Sigma = 11$ grain boundaries; the units are electrons \AA^{-3} . (a) The layer $y = 0$ for the $(1\bar{1}0)$ plane of Mg-segregated Al $\Sigma = 11(113)$ grain boundaries; (b) the layer $y = 0.5$ for the $(1\bar{1}0)$ plane of Mg-segregated Al grain boundaries (the Mg atom is shaded in grey); (c) the layer $y = 0$ for the $(1\bar{1}0)$ plane of clean grain boundaries; and (d) the layer $y = 0.5$ for the $(1\bar{1}0)$ plane of clean grain boundaries. Darker shades of grey indicate larger charge density.

Table 3. Calculated cohesive energies (eV/atom) for an Al–Mg grain boundary and a pure Al grain boundary.

	Al–Mg GB	Pure Al GB
Cohesive energy	4.157	4.266

respectively, of the plane perpendicular to the $[1\bar{1}0]$ direction for a grain boundary with Mg segregation. The total charge densities in the same layers are shown in figures 2(c) and (d) for a pure Al grain boundary. From figures 2(a) and (c), it is found that region I is an area with low charge density. In addition, the charge density in this region in the case of a Mg-contaminated boundary is lower than that of a clean boundary. Similarly, the charge density between atoms 13 and 15 (atoms 14 and 16) is lower for the grain boundary with Mg segregation than for the clean boundary. A lower charge density distribution means that Mg segregation decreases the cohesion of a boundary. In comparing figures 2(b) with (d), the area around the Mg atom with low charge density is more extended than that around Al atom 1. The bond between atoms Mg and 6 (Mg and 7) is weaker than that between atoms Al 1 and 6 (Al 1 and 7). Similarly, the bond between atoms Mg and 2 (Mg and 3) is also weaker than that between atoms Al 1 and 2

(Al 1 and 3). The charge density distribution between atoms 4 and 6, 5 and 7, 8 and 10, as well as 9 and 11, is very similar for the two boundaries. The bond between atoms 6 and 8, or 7 and 9, becomes weaker because of the existence of the Mg atom. The total charge density analysis indicates that a Mg atom has a lower binding energy than an Al at the boundary. From the above discussion, it can be concluded that the embrittlement of the grain boundary induced by Mg atoms can be attributed to the weakening of metallic bonds around the boundary plane and to the more extended low charge density region in Al–Mg grain boundaries compared with that in pure Al boundaries.

3.4. Further discussions

The calculated segregation energy demonstrates that the Mg atoms occupying the ‘looser’ sites in the plane of a boundary release larger energy than those occupying the ‘tighter’ or normal sites. The reason is that Mg occupying a ‘looser’ site leads to more local strain relaxation. From the energy or strain relaxation point of view, Mg segregation is preferred at the ‘looser’ sites in the boundary plane. Namilae *et al* [5] showed that there was a relative decrease in grain boundary energy when the Mg atom occupied the central location of a grain boundary. The first-principles calculations of this investigation explain the mechanisms of Mg segregation in a clearer manner by analysing the segregation energy and local strain relaxation.

The detrimental effect of Mg atoms on grain boundary cohesion comes from the weaker interatomic bonds between Mg and neighbouring Al atoms around a boundary plane. The region with relatively low charge density around a Mg atom also plays a crucial role in the embrittling effect of Mg on the grain boundary cohesion. The analysis of weakened metallic bonds affected by Mg atoms is helpful in understanding the mechanisms of intergranular fracture in Al–Mg alloys.

4. Summary

In this paper, the preferred sites of Mg at $\Sigma = 11(113)$ grain boundaries in Al and the effects of Mg atoms on cohesion of the boundaries have been investigated by means of first-principles plane-wave pseudopotential total energy calculations. The segregation energy calculation and local strain relaxation demonstrate that Mg prefers to occupy the ‘looser’ sites in the boundary planes. The dominant effect of Mg is to decrease the cohesive strength of a boundary and facilitate intergranular fracture.

Acknowledgments

The authors would like to thank Professor Liangyue Xiong and Professor Zhongqi Sun for very helpful discussion. This work was financially supported by the National Science Foundation of China (NSFC) (Grant No 50371087 and No 90206044) and Special Funds for the Major State Basic Research Projects of China (Grant No G2000067104).

References

- [1] Polmear I J 1995 *Light Alloys—Metallurgy of the Light Metals* 3rd edn (London: Arnold, a division of Hodder Headline PLC)
- [2] ASM 1990 *Metals Hand Book, Properties and Selection: Nonferrous Alloys and Special-Purpose Materials* 10th edn, vol 2 (Metals Park, OH: ASM International)
- [3] Na S H, Yang M S and Nam S W 1995 *Scr. Metall.* **32** 627

-
- [4] Song R G, Tseng M K, Zhang B J, Liu J, Jin Z H and Shin K S 1996 *Acta Mater.* **44** 3241
 - [5] Namila S, Chandra N and Nieh T G 2002 *Scr. Mater.* **46** 49
 - [6] Liu X Y and Adams J B 1998 *Acta Mater.* **46** 3476
 - [7] Payne M C, Teter M P, Allan D C, Arias T A and Joannopoulos J D 1992 *Rev. Mod. Phys.* **64** 1045
 - [8] Perdew J P, Chevary J A, Vosko S H, Jackson K A, Perderson M R, Singh D J and Fiolhais C 1992 *Phys. Rev. B* **46** 6671
 - [9] Vanderbilt D 1990 *Phys. Rev. B* **41** 7892
 - [10] Kleinman L and Bylander D M 1982 *Phys. Rev. Lett.* **48** 1425
 - [11] Wright A F and Atlas S R 1994 *Phys. Rev. B* **50** 15248
 - [12] Monkhorst H J and Pack J D 1977 *Phys. Rev. B* **16** 1748
 - [13] Fischer T H and Almlof J 1992 *J. Phys. Chem.* **96** 9768
 - [14] Mills M J, Daw G J, Thomas G J and Cosandey F 1992 *Ultramicroscopy* **40** 247
 - [15] Thomson D I, Heine V, Payne M C, Marzari N and Finis M W 2000 *Acta Mater.* **48** 3623
 - [16] Rice J R and Wang J S 1989 *Mater. Sci. Eng. A* **107** 23